### **ORIGINAL PAPER**



# Structural Motifs and Evolution of Boron Nanoclusters

Ekaterina D. Anisimova<sup>1</sup> · Elizaveta E. Vaneeva<sup>1,2</sup> · Vladimir S. Baturin<sup>1</sup> · Sergey V. Lepeshkin<sup>1,2</sup> · Artem R. Oganov<sup>1</sup>

Received: 22 January 2025 / Accepted: 29 March 2025 / Published online: 14 April 2025 © The Author(s), under exclusive licence to Springer Science+Business Media, LLC, part of Springer Nature 2025

#### **Abstract**

Boron is a chemically versatile element, capable of forming diverse chemical bonds (e.g., single, double, triple, 3-center 2-electron bonds, and more), which determines its chemical behavior as a pure substance and in compounds with other elements. Electron deficiency and tendency to form multicenter bonds give rise to the ubiquitous presence of clusters in structures of boron allotropes and of many boron compounds in bulk and molecular forms. Here we investigate a wide range of neutral boron clusters  $B_n$  (n = 2–60) using the first-principles evolutionary algorithm USPEX. We find clear preference for planar structures for n < 10, while there is a competition between planar, cage, bilayer, and tubular structures for n > 10. We identify magic clusters as those having positive second-order differences of the total energy (and additionally analyze their fragmentation energy and HOMO–LUMO gap). Most of the magic clusters have even n, the most notable exception being magnetic cluster  $B_{39}$  with cuboctahedral shape. Investigating the concept of aromaticity of inorganic compounds, we applied such approaches as nuclear independent chemical shift (NICS) and adaptive natural density partitioning (AdNDP) to a number of boron clusters and found that two clusters,  $B_{10}$  and  $B_{13}$ , are aromatic (the former being magic).

**Keywords** Boron clusters · USPEX · Aromaticity · Antiaromaticity · Multicenter indexes · Adaptive natural density partitioning

### Introduction

For many decades chemists, physicists and materials scientists have been attracted and fascinated by unusual bonding, unique structures and interesting properties of boron and its compounds. Boron's chemical complexity is caused by its chemical frustration, as we explained in work by Oganov and Chen et al. [1]: located between metals and nonmetals in the Periodic Table, it has only three valence electrons and therefore could be a metal, if its valence electrons were not localized so close and attracted so strongly to the nucleus. As a result of this frustration, all five established crystal structures of boron allotropes are complex [1–3]. Rhombohedral  $\beta$ -B<sub>106</sub>, which is the most common crystalline phase,

is a superhard material with a high melting point (2453 K) [4].

In the recently discovered structure of y-B28 (and likely also in  $\beta$ -B<sub>106</sub>) some boron atoms have significant fractional positive and negative charges. Due to electron deficiency of boron, multicenter covalent bonding is widespread: 3c-2e [5, 6] bonds are present within boron icosahedra in boranes and bulk boron; a 12c-2e bond has been found in the  $[B_{12}H_{12}]^{2}$ -cluster [7]. To get better understanding of such compounds, one can use the electron counting rules proposed by Wade and extended by Jemmis [8, 9]. Electron deficiency can be removed when a boron atom accepts a whole electron. According to the Zintl-Klemm [10] rule, the structural behavior of a negatively charged boron atom is similar to that of a carbon atom, which is illustrated by the structure of graphene-like boron layers observed in MgB2 [11] and in lonsdaleite-like boron framework in its predicted high-pressure phase [12].

While solid boron is non-magnetic, magnetism can appear in low-dimensional forms of this element: e.g., isolated boron atom is magnetic, and magnetic moments have



 <sup>⊠</sup> Ekaterina D. Anisimova
 Ekaterina.Anisimova@skoltech.ru

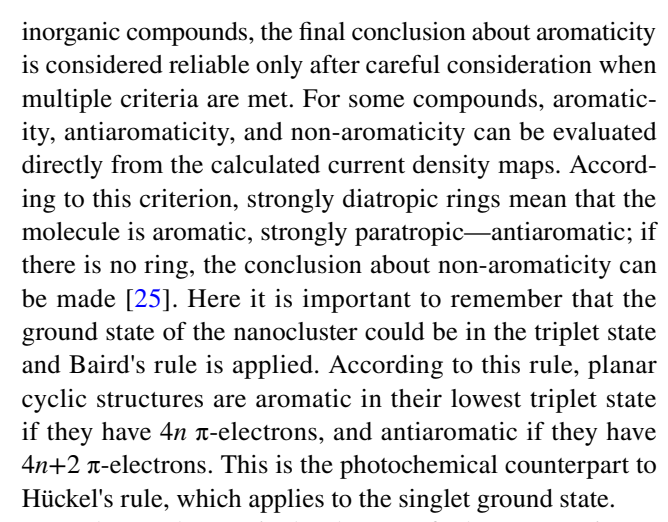
Skolkovo Institute of Science and Technology, Bolshoy Boulevard 30, bld. 1, Moscow 121205, Russia

Lebedev Physical Institute, Russian Academy of Sciences, 119991 Leninsky Ave. 53, Moscow, Russia

been predicted in some low-energy forms of borophene [13]. Some boron clusters can be magnetic as well.

Boron nanoclusters get increasing attention due to their potentially interesting electronic and chemical (e.g., catalytic) properties. Boron-containing compounds are widely utilized in luminescent materials, liquid crystals, polymers, sensors, nonlinear optics, and coordination polymers. In addition to these applications, boron is notable for its exceptionally high gravimetric and volumetric energy densities (for example, in combustion processes) among elements. This makes it a valuable additive to traditional hydrocarbon fuels, such as n-decane and kerosene, to enhance their energy density and improve combustion efficiency. Boron can significantly increase the combustion temperature due to its high heat of combustion, resulting in improved thermal efficiency and greater thrust or energy output of the fuel. While crystalline boron allotropes contain icosahedral B<sub>12</sub> groups, structures of small boron nanoclusters are quite different [14]. So, it is interesting to find at which size boron clusters become similar to the structures of bulk boron allotropes. Pure boron nanoparticles are expected to form singleatom planar sheets, cages, or nanotubes, which has been confirmed by many theoretical and experimental studies. The preferred geometry (planar [14], tubular [14–16], bilayer [17], cage [17], and core-shell [18]) depends on the cluster size. Small clusters (with up to 20 atoms) have been mostly found to exist in planar configurations [19, 20]. In mediumsized clusters, there is a competition between two structural motifs [17, 21]. For example, the well-known quasi-planar structure B<sub>36</sub> is known from experiment and is thought as a building block for producing a single-atom borophene sheet [22]. The smallest tubular boron structure seen in the experiment consists of 20 atoms and is a potential precursor for single-walled boron nanotubes [22]. Boron cages have also been subject of great interest, with B<sub>40</sub> being the first synthesized. Accurate calculations have confirmed that clusters containing 46, 48, and 50 atoms exist in three competitive structures: core-shell, bilayer, and quasi-planar [17]. Larger clusters have been demonstrated to form core-shell, rather than hollow-cage structures [18]. First-principles studies of B<sub>80</sub>, B<sub>68</sub>, and B<sub>74</sub> have established the existence of a B<sub>12</sub> icosahedral core which makes the core-shell geometry more stable than cage [18]. These large clusters can be viewed as already reminiscent of the structures of bulk boron allotropes.

An interesting and for now elusive aspect of inorganic molecules and nanoclusters is aromaticity. The very concept of aromaticity is rather ambiguous, and has led to six criteria [23] to determine if a compound is aromatic, nonaromatic, or antiaromatic (i.e., having  $4n \pi$ -electrons that destabilize cyclic systems and make them more reactive [24]): electronic, energetic, geometric, magnetic, and the ones based on reactivity and spectroscopy. In the case of



For boron clusters, in the absence of relevant experimental data, only four criteria can be evaluated—magnetic, spectroscopic, bonding analysis, and resonance energy. Similar approach to assess structural evolution and stability was used in a number of previous works [26–30]. In this work, we want to get a full understanding of the  $B_n$  clusters' behavior through an investigation of their optimal and low-energy metastable structures in a wide range of compositions (n = 2-60). Structural competition and evolution as a function of the number of atoms were investigated and compared with the previously reported results. Another goal of our study is to determine magic clusters (and factors stabilizing them), explore the evolution of the type of structure with increasing number of atoms, and check the possible effect of aromaticity on stabilization of clusters.

# **Computational Details**

The initial search for lowest-energy boron clusters was performed using the first-principles evolutionary algorithm USPEX [21, 31, 32]. This method offers an important advantage of enabling simultaneous prediction of structures of different composition, taking advantage of their evolutionary competition and exchange of structural information. This leads to a significant speedup of the calculations, relative to traditional approach of predicting structures for each composition separately [33]. Our approach allows one to efficiently determine not only the ground-state structures for each composition, but also many low-energy isomers, which allows one to study competition between different structure types.

The local geometry relaxations during global optimization search were performed within density functional theory (DFT) using PAW method [34] and Perdew–Burke–Ernzerhof (PBE) functional [35], as implemented in the VASP code [36, 37]. Subsequently, the 10 lowest-energy isomers from each composition were selected for further refinement using the GAUSSIAN software [38], applying the



PBE0 hybrid functional [39] and the Def2-TZVPP basis set [40], finding spin multiplicity corresponding to lower electronic state (M=1, M=2 or M=3). All energetic characteristics and HOMO-LUMO gaps were calculated using the same level of theory.

To identify particularly stable clusters, expected to have particularly high abundances, we computed the second-order differences in the total energies  $\Delta^2 E$ . As additional criteria, we used the fragmentation energies and HOMO–LUMO gaps. We also investigated the aromaticity in boron clusters following different criteria that can be evaluated for inorganic compounds: adaptive natural density partitioning method (AdNDP) [41–45], and nuclear independent chemical shift (NICS) [46].

### **Results and Discussion**

### **Structure**

All predicted clusters were divided into the planar, cage, tubular, core–shell, and bilayer groups. A cluster is considered planar when all its atoms lie approximately in the same plane. Another type is tubular clusters, including clusters with one or two atoms sticking out of the tube. Three-dimensional structures consisting of a shell and core containing fewer than five atoms were classified as cage structures. Structures consisting of two connected planes were classified as bilayer ones. Finally, boron shells encapsulating an icosahedral B<sub>12</sub> core were classified as core–shell structures. These five types were discerned among 5100 structures of boron clusters containing from 10 to 60 atoms (50 different

compositions with 100 isomers for each) that were found through evolutionary search.

All obtained ground-state structures of  $B_n$  clusters (n =2—60) are shown in Fig. 1. The xyz coordinates of all calculated ground-state structures are provided in ESI Section S2. The clusters, containing 3-5, 8, 10, 11, 13, 15-18 atoms are planar, clusters with 6, 7, 9, 12, 23 and 36 atoms are quasiplanar (exhibit a nearly planar geometry with slight deviations), all the rest are attributed to non-planar clusters. For further study, we have selected clusters containing 10-60 atoms, where the structure competition occurs. For these structures, we looked at the structural tendencies of boron cluster isomers (Fig. 2) as a function of structural patterns from the number of atoms in each cluster plotted as energy difference between structures and their ground states. Boron clusters with 10-20 atoms adapt mostly planar structure with exceptions of  $B_{14}$ ,  $B_{19}$ , which are cage, and tubular  $B_{20}$ .  $B_n$ clusters with n = 21-40 showed the tendency to be cage with the exception of tubular B<sub>21</sub>, quasi-planar B<sub>23</sub> and B<sub>36</sub>, the latter being highly symmetric. Clusters with 41-60 atoms usually are bilayer, except  $B_{41}$  in cage form and  $B_{59}$  with core-shell structure.

Our results on the structural competition agree with those previously reported.[19–21, 47, 48] The remarkable magnetic cluster  $B_{39}$ , first found by Wu and colleagues [21] and characterized by a highly symmetric cage  $(O_h)$  of 38 atoms around the central boron atom, was also predicted in our calculations.

For compositions  $B_{31}$ ,  $B_{32}$ ,  $B_{33}$ ,  $B_{35}$ ,  $B_{37}$ ,  $B_{38}$ ,  $B_{41}$ ,  $B_{43}$ ,  $B_{44}$ ,  $B_{45}$ ,  $B_{49}$  and  $B_{50}$  we identified ground-state structures not previously described in the literature.[21] These clusters exhibit lower energy by ~0.3–1.2 eV and mostly have low-symmetry structures, except  $B_{50}$  with  $D_{2d}$  symmetry.

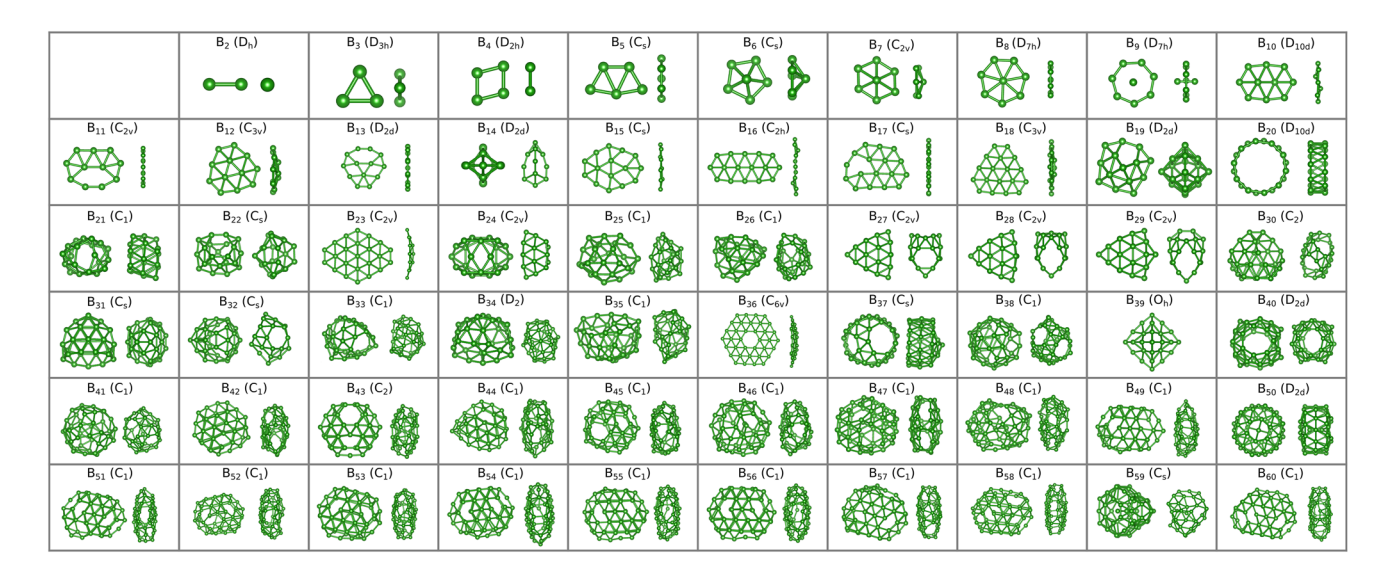


Fig. 1 Ground-state structures of  $B_n$  clusters (n = 2-60) in two projections with their point groups



**98** Page 4 of 9 E. D. Anisimova et al.

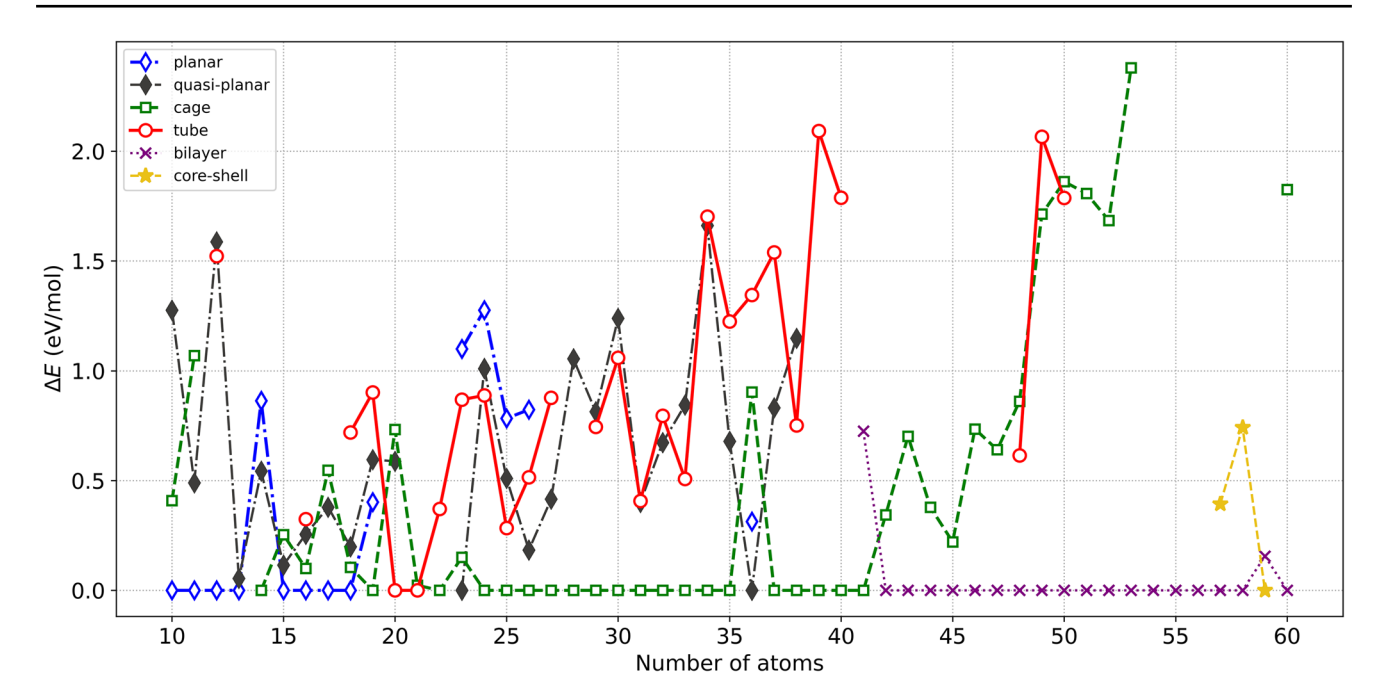


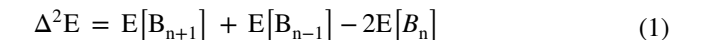
Fig. 2 Structural competition in the  $B_n$  clusters (n = 10–60). Vertical axis represents  $\Delta E$  between different structures and the most stable structure at each atomic composition n.

Indeed, lowest-energy structures are not always bound to demonstrate high symmetry, and USPEX algorithm is capable of discovering such clusters.

### **Energetics**

One should remember that any cluster is higher in energy than its infinite periodic counterpart—the bulk crystal, and therefore stability of clusters should be discussed not in terms of the lowest possible energy, but using local criteria (comparing a given cluster with clusters of similar size). Second-order differences in the total energy  $\Delta^2 E$  have been shown to work well for this purpose [49, 50], while additional insight is also provided by the fragmentation energy (the minimum energy required to split a given cluster into two smaller clusters) and the HOMO–LUMO gap. In addition to evaluating stability of our clusters, we were interested in the trends—spin states (singlet, doublet or triplet), point group symmetries, and wanted to know how our results agree with previous studies [19–21, 47, 48, 51].

These criteria of stability have been successfully used in our previous studies [33, 52–59]. In the first criterion, we consider the stability with respect to the exchange of one boron between two identical nanoclusters  $B_n$ . This corresponds to the so-called second energy difference (discrete analog of the second derivative of the energy) and can be written as:



A cluster with n atoms is considered stable ("magic") when two clusters B<sub>n</sub> have lower energy than two clusters of neighboring compositions— $B_{n+1}$  and  $B_{n-1}$ . Physically, this means that a collision of two such clusters will not lead to transfer of an atom from one cluster to the other, and such clusters can accumulate in significant concentrations. Mathematically, such stability is expressed by positive second-order energy difference  $\Delta^2 E$ , which reveals 30 "magic" boron clusters (Fig. 3a), most of which have even numbers of boron atoms (and, consequently, even numbers of electrons). The magic clusters  $B_n$  with n = 4, 10, 12, 14, 16, 18, 20, 22,24, 28, 30, 32, 34, 36, 40, 46, 52, 54, 56, 58 are in the singlet state, those with n = 3, 5, 7, 27, 39, 43, 49, 51, 59 have an odd number of electrons (i.e., are open-shell and magnetic), and are in the doublet state, and the unique case n = 8 corresponds to a cluster with an even number of electrons in the triplet state. Total energies and magnetic moments are given in Section 1, Table S2, Supplementary Information.

Additionally, we have used the second criterion—the HOMO–LUMO gap. A wide HOMO–LUMO gap is usually associated with increased stability, but it is not expected to be completely correlated with  $\Delta^2 E$ . The HOMO–LUMO gaps (Fig. 3b) have particularly high values for the following eleven magic clusters:  $B_3$ ,  $B_4$ ,  $B_6$ ,  $B_8$ ,  $B_9$ ,  $B_{12}$ ,  $B_{14}$ ,  $B_{24}$ ,  $B_{30}$  and  $B_{40}$ . Wide HOMO-LUMO gaps are related to low electronic polarizability, which implies relatively low reactivity and high kinetic stability.



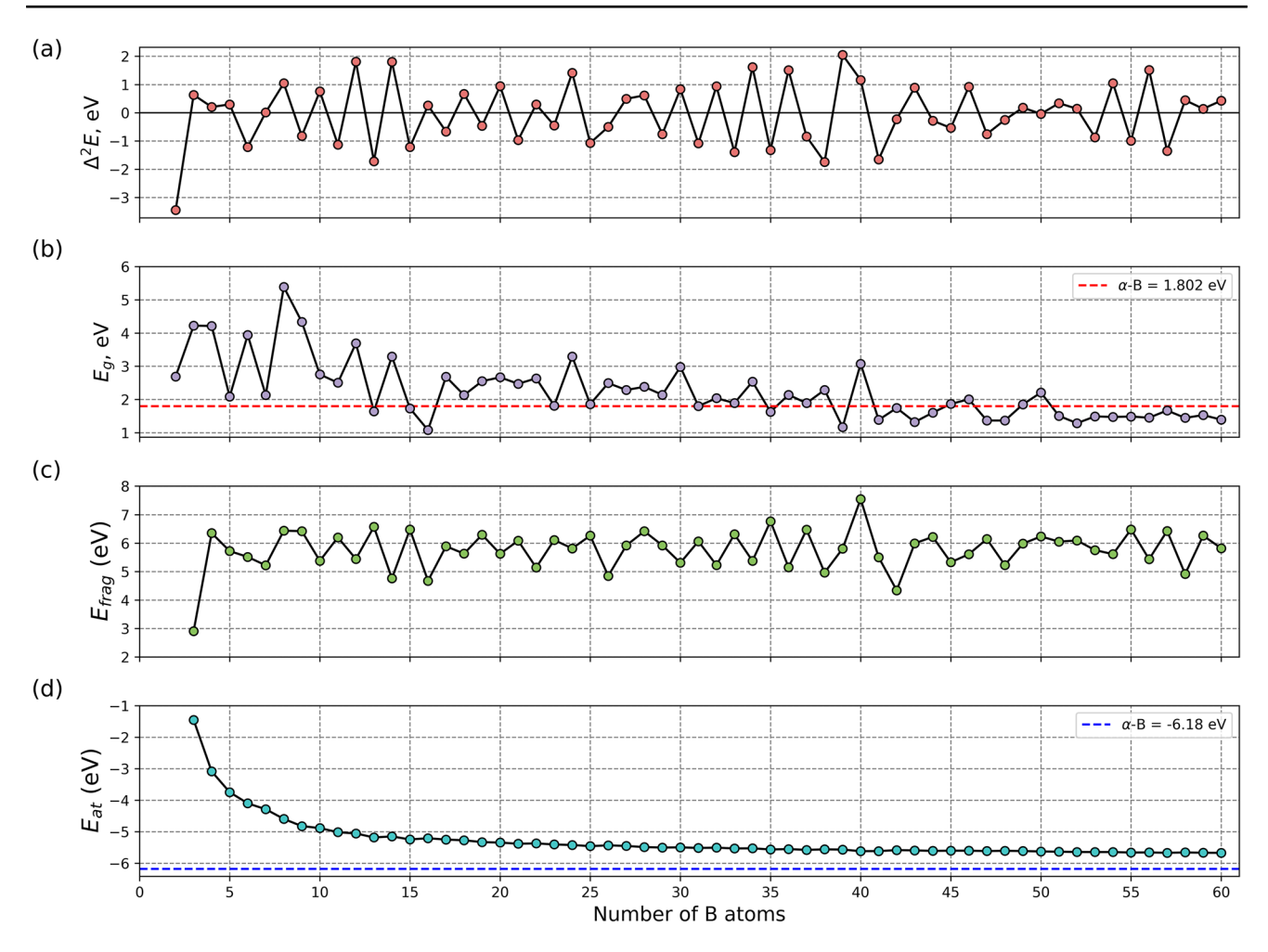


**Fig. 3** a Second-order differences of energy  $\Delta^2 E$ , **b** HOMO-LUMO gaps, **c** fragmentation energies  $\Delta E_{\rm frag}$  and **d** atomization energies  $E_{\rm at}$  of the ground-state structures of the B<sub>n</sub> clusters (n=2-60). The theoretical band gap of  $\alpha$ -boron is equal to 1.802 eV, and the calcu-

lated atomization energy of crystalline  $\alpha$ -B is -6.18 eV; one can see how the band gaps and atomization energies of large boron clusters asymptotically approach bulk values.

Another stability criterion characterizes resistance to fragmentation. Here we identify molecules that could spontaneously decompose. To this end, we consider all possible channels of fragmentation of a given molecule for the decomposition into two fragments:

$$B_n = B_{n-a} + B_a$$
, where  $0 \le a \le n$  (2)

The energy of each fragmentation reaction  $n \rightarrow a + (n-a)$  is found as:

$$E_{\text{frag},}(n,a) = E(a) + E(n-a) - E(n)$$
(3)

We are looking for the decomposition into the most stable fragments, hence, we calculated the minimal value of all fragmentation energies:

$$E_{\text{frag}}(n) = \min_{a} E_{\text{frag}}(n, a) \tag{4}$$

Interestingly, the lowest-energy fragmentation path for all boron clusters is the removal of one boron atom. The dependence of the fragmentation energy on the number of atoms is shown in Fig. 3c. Again, we see that clusters with even numbers of boron atoms tend to have particularly high fragmentation energies. Interestingly, clusters with high energy of removal of one boron atom also have high values of  $\Delta^2 E$  (the exception is  $B_{23}$  with high  $E_{\rm frag}$  and nearly zero  $\Delta^2 E$ ). The energy of removal of one B atom is the structural analog of the ionization potential (energy of removal of one electron). Its high values are indicative of a closed structural shell.

To obtain a full picture, the atomization energy (Fig. 4d) was calculated using the formula:

$$E_{\text{at}}(n) = \left( E[\mathbf{B}_n] - nE[\mathbf{B}_1] \right) / n, \tag{5}$$

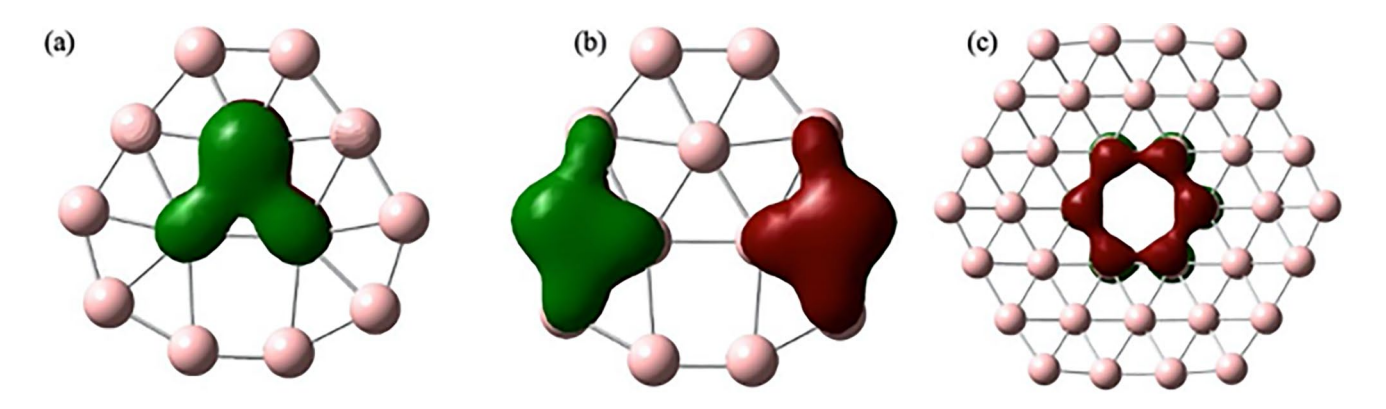


Fig. 4 AdNDP analysis of a 3c-2e and b 4c-2e bonds of  $B_{13}$ , and c 6c-2e bond of  $B_{36}$ 

where  $E[B_1]$  is the energy of an isolated boron atom,  $E[B_n]$  is the total energy of the cluster, and n is the number of atoms. As expected,  $E_{\rm at}$  decreases with the number of atoms, approaching the bulk value, and bulk crystal has lower energy than any cluster.

Summarizing the results analyzed above, energetic criteria show that mostly even-numbered clusters are showing special stability. These are  $B_8,\,B_{10},\,B_{12},\,B_{14},\,B_{20},\,B_{24},\,B_{30},\,B_{32},\,B_{34},\,B_{36},\,B_{40}$ . It is worth mentioning that  $B_8$  has a triplet ground state, and hence, due to Baird's rule, is aromatic (has  $4n\,\pi$ -electrons). The symmetry of magic clusters is higher than that of the neighboring non-magic ones. Magicity stems from closed electronic and/or structural shell—the former implies singlet state, whereas the latter implies high symmetry.

### **Aromaticity**

Aromaticity is an important property of a molecular cluster that can often be understood by analyzing the characteristic features of its individual fragments [60]. In some cases, the overall aromaticity of a system can be approximated as the sum of the aromaticities of its constituent parts. In this study, we aim to explore the relationship between aromaticity and magicity in boron clusters by analyzing both magic and non-magic species. Specifically, we selected several representative clusters ( $B_{10}$ ,  $B_{11}$ ,  $B_{12}$ ,  $B_{13}$ ,  $B_{15}$ ,  $B_{16}$ ,  $B_{18}$  and  $B_{36}$ ) to determine whether their stability (magicity) correlates with their possibly aromatic character.

To assess aromaticity, we employed the Nuclear Independent Chemical Shift (NICS) method [46], which falls under the magnetic criteria of aromaticity introduced by Paul v. R. Schleyer in 1996. The NICS approach is based on the response of an aromatic system to an external magnetic field, allowing for the quantification of aromatic character. For the selected boron clusters, we computed NICS values at their geometric centers to determine the extent of electron delocalization, which is often associated with enhanced

stability. If a cluster exhibits a significant negative NICS value, it suggests a strong aromatic character due to electron delocalization in closed circuits.

Our results presented in Table 1 reveal that, among the studied clusters, only  $B_{10}$  and  $B_{13}$  exhibit negative NICS values, indicating their aromatic nature. Interestingly, despite its pronounced aromaticity,  $B_{13}$  is classified as a non-magic cluster, suggesting that aromaticity has very limited effect here and alone does not necessarily dictate the overall stability of boron clusters.  $B_{10}$  is both aromatic and magic.

In addition to NICS analysis, we applied the Adaptive Natural Density Partitioning (AdNDP) method to further investigate the electronic structure and bonding patterns within these clusters. AdNDP provides an insightful representation of molecular bonding by identifying localized and delocalized electron pairs. The method systematically recovers traditional Lewis bonding elements (such as 1c-2e and 2c-2e bonds) while also revealing multicenter delocalized bonding patterns (for n > 2), which are strongly linked to aromaticity.

As shown in Fig. 4, our AdNDP analysis of B<sub>13</sub> highlights the presence of multicenter 3c–2e and 4c–2e bonds, reinforcing its aromatic character. Meanwhile, B<sub>36</sub> features a prominent 6c–2e bond, suggesting delocalization effects that may contribute to its stability.

**Table 1** Calculated NICS values of corresponding clusters at the geometry center, 1 Å and 2 Å above were computed, given in ppm.

Cluster	NICS(0)	NICS(1)	NICS(2)
B <sub>10</sub>	- 52.836	- 21.097	- 4.168
$B_{11}$	25.995	19.158	7.912
$B_{12}$	27.743	14.385	8.541
B <sub>13</sub>	- 12.363	- 8.439	- 7.695
B <sub>15</sub>	15.660	11.592	2.944
B <sub>16</sub>	24.012	15.898	5.827
B <sub>18</sub>	25.683	21.897	6.731



Overall, our findings suggest that while aromaticity plays a role in the electronic structure and bonding of boron clusters, it does not always correlate directly with their magicity.

# **Conclusions**

In this study, we investigated a wide range of boron clusters and identified clear trends in their structural motifs. As the number of atoms increases from 10 to 60, boron clusters predominantly adopt planar, cage, or bilayer structures, with only a few tubular structures observed. For clusters containing more than 60 atoms, structural diversity diminishes, and core-shell structures become the only motif present, resembling bulk boron structures. We identified previously undescribed ground-state structures for the compositions B<sub>31</sub>, B<sub>32</sub>, B<sub>33</sub>, B<sub>35</sub>, B<sub>37</sub>, B<sub>38</sub>, B<sub>41</sub>, B<sub>43</sub>, B<sub>44</sub>, B<sub>45</sub>, B<sub>49</sub>, and B<sub>50</sub>. These newly identified structures are ~0.3–1.2 eV lower in energy compared to alternatives reported in the literature, and most exhibit low symmetry, with the exception of B<sub>50</sub>, which exhibits D<sub>2d</sub> symmetry. To evaluate stability of the clusters, we employed a simple approach by calculating the second derivative of the cluster energy with respect to composition. This analysis revealed magic clusters, including B<sub>8</sub>,  $B_{10}$ ,  $B_{12}$ ,  $B_{14}$ ,  $B_{20}$ ,  $B_{24}$ ,  $B_{30}$ ,  $B_{32}$ ,  $B_{34}$ ,  $B_{36}$ , and  $B_{40}$  and some others. The symmetry of these magic clusters is generally higher than that of their non-magic neighbors. Notably, B<sub>o</sub> has a triplet ground state and is aromatic due to Baird's rule, possessing  $4n \pi$ -electrons. To further investigate, we tested the concept of aromaticity on several magic  $B_n$  clusters (n = 10–60) using a nuclear independent shift approach. Our findings indicate that only two clusters, B<sub>10</sub> and B<sub>13</sub>, are aromatic, with B<sub>10</sub> being the only one classified as magic. Thus, aromaticity plays a minor role in the stabilization of boron clusters (magicity). Instead, the dominant factors are a closed-shell electronic structure, characterized by large HOMO-LUMO gaps and an even number of electrons, and a closed-shell atomic structure.

Supplementary Information The online version contains supplementary material available at https://doi.org/10.1007/s10876-025-02815-0.

Acknowledgements This work was supported by the Russian Science Foundation (grant #19-72-30043). The calculations were performed on Oleg and Arkuda supercomputers at Skoltech and at the Joint Supercomputer Center of Russian Academy of Sciences, the Lobachevsky cluster at the University of Nizhny Novgorod and supercomputer "Govorun" at JINR.

Author contributions Ekaterina D. Anisimova—conceptualization, data curation, validation, visualization, writing—the original draft, and writing—review and editing. Elizaveta E. Vaneeva—global optimization, data curation, validation, methodology and writing—review and editing. Vladimir S. Baturin—formal analysis, investigation, and writing—review and editing. Sergey V. Lepeshkin—nvestigation, validation, methodology and writing—review and editing. A. R.

Oganov—conceptualization, writing—review and editing, and supervision. All co-authors contributed to the discussion of the data. All authors have given approval to the final version of the manuscript.

Data availability No datasets were generated or analysed during the current study.

### **Declarations**

**Conflict of interest** The authors declare no competing interests.

#### References

- A. R. Oganov, et al. (2009). Ionic high-pressure form of elemental boron. *Nature* 457 (7231), 863–867. https://doi.org/10.1038/nature07736.
- A. Masago, K. Shirai, and H. Katayama-Yoshida (2006). Crystal stability ofα- andβ-boron. *Phys Rev B Condens Matter Mater Phys.* https://doi.org/10.1103/physrevb.73.104102.
- E. A. Ekimov and I. P. Zibrov (2011). High-pressure high-temperature synthesis and structure of α-tetragonal boron. *Sci Technol Adv Mater* 12 (5), 055009. https://doi.org/10.1088/1468-6996/12/5/055009.
- C. Housecroft, *Inorganic Chemistry*. Pearson Higher Ed, 2018. [Online]. Available: https://books.google.com/books/about/Inorganic\_Chemistry.html?hl=&id=A8hdDwAAQBAJ
- R. Kawai and J. H. Weare (1991). Instability of the B12 icosahedral cluster: Rearrangement to a lower energy structure. *J. Chem. Phys.* 95 (2), 1151–1159. https://doi.org/10.1063/1.461145.
- E. D. Jemmis and D. L. V. K. Prasad (2006). Icosahedral B12, macropolyhedral boranes, β-rhombohedral boron and boron-rich solids. J. Solid State Chem. 179 (9), 2768–2774. https://doi.org/ 10.1016/j.jssc.2005.11.041.
- J. A. Wunderlich and W. N. Lipscomb (1960). Structure of B<sub>12</sub>H<sub>12</sub>-<sup>2</sup> ION. J. Am. Chem. Soc. 82 (16), 4427–4428. https://doi.org/10.1021/ja01501a076.
- E. D. Jemmis and M. M. Balakrishnarajan (2001). Polyhedral boranes and elemental boron: direct structural relations and diverse electronic requirements. *J Am Chem Soc* 123 (18), 4324– 4330. https://doi.org/10.1021/ja0026962.
- E. D. Jemmis, M. M. Balakrishnarajan, and P. D. Pancharatna (2001). A unifying electron-counting rule for macropolyhedral boranes, metallaboranes, and metallocenes. *J Am Chem Soc* 123 (18), 4313–4323. https://doi.org/10.1021/ja003233z.
- A. V. Shevelkov and K. Kovnir, Zintl Clathrates, in V. Shal (ed.), Zintl Phases in Structure and bonding (Springer, Heidelberg, 2010), pp. 97–142. https://doi.org/10.1007/430\_2010\_25.
- J. Nagamatsu, N. Nakagawa, T. Muranaka, Y. Zenitani, and J. Akimitsu (2001). Superconductivity at 39 K in magnesium diboride. *Nature* 410 (6824), 63–64. https://doi.org/10.1038/35065039.
- 12. Y. Ma, Y. Wang, and A. R. Oganov (2009). Absence of super-conductivity in the high-pressure polymorph of MgB2. *Phys Rev B Condens Matter Mater Phys.* https://doi.org/10.1103/physrevb. 79.054101.
- A. J. Mannix, et al. (2015). Synthesis of borophenes: anisotropic, two-dimensional boron polymorphs. *Science* 350 (6267), 1513– 1516. https://doi.org/10.1126/science.aad1080.
- B. Kiran, S. Bulusu, H.-J. Zhai, S. Yoo, X. C. Zeng, and L.-S. Wang (2005). Planar-to-tubular structural transition in boron clusters: B20 as the embryo of single-walled boron nanotubes. *Proc Natl Acad Sci U S A* 102 (4), 961–964. https://doi.org/10.1073/pnas.0408132102.



- I. V. Zaporotskova, E. V. Perevalova, and N. P. Zaporotskova, "Boron nanotubes and their properties: semiempirical investigation," in ESOMAT 2009 - 8th European Symposium on Martensitic Transformations, Les Ulis, France: EDP Sciences, 2009. https://doi.org/10.1051/esomat/200902037.
- J. Wang, H.-Y. Zhao, and Y. Liu (2014). Boron-double-ring sheet, fullerene, and nanotubes: potential hydrogen storage materials. *Chemphyschem* 15 (16), 3453–3459. https://doi.org/ 10.1002/cphc.201402418.
- 17. L. Sai, X. Wu, N. Gao, J. Zhao, and R. B. King (2017). Boron clusters with 46, 48, and 50 atoms: competition among the coreshell, bilayer and quasi-planar structures. *Nanoscale* **9** (37), 13905–13909. https://doi.org/10.1039/c7nr02399e.
- J. Zhao, L. Wang, F. Li, and Z. Chen (2010). B(80) and other medium-sized boron clusters: core-shell structures, not hollow cages. *J Phys Chem A* 114 (37), 9969–9972. https://doi.org/10. 1021/jp1018873.
- M. Atiş, C. Özdoğan, and Z. B. Güvenç (2007). Structure and energetic of B<sub>n</sub> (n = 2–12) clusters: Electronic structure calculations. *Int. J. Quantum Chem.* 107 (3), 729–744. https://doi.org/10.1002/qua.21171.
- T. B. Tai, N. M. Tam, and M. T. Nguyen (2012). Structure of boron clusters revisited, Bn with n=14-20. *Chem. Phys. Lett.* 530, 71-76. https://doi.org/10.1016/j.cplett.2012.01.039.
- 21. X. Wu, et al. (2020). Competition between tubular, planar and cage geometries: a complete picture of structural evolution of B (n = 31–50) clusters. *Phys Chem Chem Phys* **22** (23), 12959–12966. https://doi.org/10.1039/d0cp01256d.
- Z. A. Piazza, H.-S. Hu, W.-L. Li, Y.-F. Zhao, J. Li, and L.-S. Wang (2014). Planar hexagonal B(36) as a potential basis for extended single-atom layer boron sheets. *Nat Commun* 5, 3113. https://doi.org/10.1038/ncomms4113.
- T. R. Galeev and A. I. Boldyrev, Aromaticity and antiaromaticity in inorganic chemistry, Comprehensive inorganic chemistry II. Elsevier, Amsterdam, pp 245–275. https://doi.org/10.1016/b978-0-08-097774-4.00909-8.
- V. I. Minkin (1999). Glossary of terms used in theoretical organic chemistry. *Pure Appl. Chem.* 71 (10), 1919–1981. https://doi.org/10.1351/pac199971101919.
- I. A. Popov and A. I. Boldyrev, Chemical bonding in inorganic aromatic compounds, The chemical bond. (Wiley-VCH Verlag GmbH & Co. KGaA, Weinheim, 2014), pp. 421–444. https:// doi.org/10.1002/9783527664658.ch14.
- F. Li, et al. (2012). B80 and B101–103 clusters: remarkable stability of the core-shell structures established by validated density functionals. *J Chem Phys* 136 (7), 074302. https://doi.org/10.1063/1.3682776.
- 27. C. Li, et al. (2021). A density functional investigation on the structures, electronic, spectral and fluxional properties of VB20-cluster. *J. Mol. Liq.* **339** (116764), 116764. https://doi.org/10.1016/j.molliq.2021.116764.
- 28. C.-G. Li, et al. (2020). Analysis of the structures, stabilities and electronic properties of MB16–(M = V, Cr, Mn, Fe Co, Ni) clusters and assemblies. *New J Chem* **44** (13), 5109–5119. https://doi.org/10.1039/c9nj06335h.
- 29. C.-G. Li, et al. (2019). A comparative study of CunX (X = Sc, Y; n = 1–10) clusters based on the structures, and electronic and aromatic properties. *New J Chem* **43** (17), 6597–6606. https://doi.org/10.1039/c9nj00236g.
- C. Li, et al. (2021). Systematic investigation of geometric structures and electronic properties of lithium doped magnesium clusters. *Comput. Mater. Sci.* 200 (110800), 110800. https://doi.org/10.1016/j.commatsci.2021.110800.
- 31. A. R. Oganov and C. W. Glass (2006). Crystal structure prediction using ab initio evolutionary techniques: principles and

- applications. J. Chem. Phys. **124** (24), 244704. https://doi.org/10.1063/1.2210932.
- A. R. Oganov, A. O. Lyakhov, and M. Valle (2011). How evolutionary crystal structure prediction works—and why. Acc. Chem. Res. 44 (3), 227–237. https://doi.org/10.1021/ar1001318.
- S. V. Lepeshkin, V. S. Baturin, Y. A. Uspenskii, and A. R. Oganov (2019). Method for Simultaneous Prediction of Atomic Structure and Stability of Nanoclusters in a Wide Area of Compositions. *J. Phys. Chem. Lett.* 10 (1), 102–106. https://doi.org/10.1021/acs.ipclett.8b03510.
- P. E. Blöchl (1994). Projector augmented-wave method. *Phys. Rev. B Condens. Matter* 50 (24), 17953–17979. https://doi.org/10.1103/physrevb.50.17953.
- 35. J. P. Perdew, K. Burke, and M. Ernzerhof (1996). Generalized gradient approximation made simple. *Phys. Rev. Lett.* **77** (18), 3865–3868. https://doi.org/10.1103/PhysRevLett.77.3865.
- G. Kresse and J. Furthmüller (1996). Efficient iterative schemes for ab initio total-energy calculations using a plane-wave basis set. *Phys. Rev. B Condens. Matter* 54 (16), 11169–11186. https://doi. org/10.1103/physrevb.54.11169.
- G. Kresse and J. Hafner (1993). Ab initio molecular dynamics for liquid metals. *Phys. Rev. B Condens. Matter* 47 (1), 558–561. https://doi.org/10.1103/physrevb.47.558.
- P. J. Stephens, F. J. Devlin, C. F. Chabalowski, and M. J. Frisch (1994). Ab initio calculation of vibrational absorption and circular dichroism spectra using density functional force fields. *J. Phys. Chem.* 98 (45), 11623–11627. https://doi.org/10.1021/j1000 963001
- C. Adamo and V. Barone (1999). Toward reliable density functional methods without adjustable parameters: The PBE0 model.
   J. Chem. Phys. 110 (13), 6158–6170. https://doi.org/10.1063/1.478522.
- A. Hellweg and D. Rappoport (2015). Development of new auxiliary basis functions of the Karlsruhe segmented contracted basis sets including diffuse basis functions (def2-SVPD, def2-TZVPPD, and def2-QVPPD) for RI-MP2 and RI-CC calculations. *Phys Chem Chem Phys* 17 (2), 1010–1017. https://doi.org/10.1039/c4cp04286g.
- T. M. Krygowski and M. K. Cyrański (2001). Structural aspects of aromaticity. *Chem Rev* 101 (5), 1385–1419. https://doi.org/10. 1021/cr990326u.
- P. F. Weck, A. P. Sergeeva, E. Kim, A. I. Boldyrev, and K. R. Czerwinski (2011). Chemical bonding and aromaticity in trinuclear transition-metal halide clusters. *Inorg Chem* 50 (3), 1039–1046. https://doi.org/10.1021/ic101779w.
- D. M. Bishop, M. Chaillet, K. Larrieu, and C. Pouchan (1984).
   Some electrical properties of Li3 + and Li3 -. *Mol. Phys.* 51 (1), 179–183. https://doi.org/10.1080/00268978400100131.
- A. P. Sergeeva and A. I. Boldyrev (2010). δ-Bonding in the [Pd4(μ4-C9H9)(μ4-C8H8)]+ sandwich complex. *Phys Chem Chem Phys* 12 (38), 12050–12054. https://doi.org/10.1039/c0cp0 0475h.
- A. N. Alexandrova and A. I. Boldyrev (2003). Σ-aromaticity and σ-antiaromaticity in alkali metal and alkaline earth metal small clusters. *J. Phys. Chem. A* 107 (4), 554–560. https://doi.org/10.1021/jp027008a.
- Z. Chen, C. S. Wannere, C. Corminboeuf, R. Puchta, and P. R. von Schleyer (2005). Nucleus-independent chemical shifts (NICS) as an aromaticity criterion. *Chem Rev* 105 (10), 3842–3888. https:// doi.org/10.1021/cr030088.
- T. B. Tai and M. T. Nguyen (2015). Electronic structure and photoelectron spectra of Bn with n = 26–29: an overview of structural characteristics and growth mechanism of boron clusters. *Phys Chem Chem Phys* 17 (20), 13672–13679. https://doi.org/10.1039/c5cp01851j.



- 48. H.-J. Zhai, et al. (2014). Observation of an all-boron fullerene. *Nat Chem* **6** (8), 727–731. https://doi.org/10.1038/nchem.1999.
- X. Liu, G.-F. Zhao, L.-J. Guo, Q. Jing, and Y.-H. Luo (2007). Structural, electronic, and magnetic properties of MBn(M=Cr, Mn, Fe Co, Ni, n≤7) clusters. *Phys Rev A*. https://doi.org/10.1103/ physreva.75.063201.
- 50. M. Böyükata and Z. B. Güvenç (2011). Density functional study of AlBn clusters for n=1-14. *J. Alloys Compd.* **509** (11), 4214–4234. https://doi.org/10.1016/j.jallcom.2011.01.053.
- K. Ge Cheng, et al. (2024). Probing the structural evolution, electronic and vibrational properties of neutral and anionic potassium-doped magnesium clusters. *Results Phys.* 65, 107954. https://doi.org/10.1016/j.rinp.2024.107954.
- H. J. Novinsky, R. Pflaum, P. Pfau, K. Sattler, and E. Recknagel (1985). Mass spectrometric studies on lead compound clusters. Surf. Sci. 156, 126–133. https://doi.org/10.1016/0039-6028(85) 90565-5.
- 53. X. Xing, Z. Tian, H. Liu, and Z. Tang (2003). Magic bimetallic cluster anions of M/Pb (M = Au, Ag and Cu) observed and analyzed by laser ablation and time-of-flight mass spectrometry. *Rapid Commun. Mass Spectrom.* 17 (13), 1411–1415. https://doi.org/10.1002/rcm.1063.
- 54. D. V. Rybkovskiy, S. V. Lepeshkin, A. A. Mikhailova, V. S. Baturin, and A. R. Oganov (2024). Lithiation of phosphorus at the nanoscale: a computational study of LiP clusters. *Nanoscale* **16** (3), 1197–1205. https://doi.org/10.1039/d3nr05166h.
- V. Rybkovskiy, S. V. Lepeshkin, V. S. Baturin, A. A. Mikhailova, and A. R. Oganov (2023). Phosphorus nanoclusters and insight into the formation of phosphorus allotropes. Nanoscale 15 (3), 1338–1346. https://doi.org/10.1039/d2nr06523a.
- A. A. Mikhailova, S. V. Lepeshkin, V. S. Baturin, A. P. Maltsev,
   Y. A. Uspenskii, and A. R. Oganov (2023). Ultralow reaction

- barriers for CO oxidation in Cu-Au nanoclusters. *Nanoscale* **15** (33), 13699–13707. https://doi.org/10.1039/d3nr02044d.
- M. Fedyaeva, S. Lepeshkin, and A. R. Oganov (2023). Stability of sulfur molecules and insights into sulfur allotropy. *Phys. Chem. Chem. Phys.* 25 (13), 9294–9299. https://doi.org/10.1039/d2cp0 5498a.
- E. E. Vaneeva, S. V. Lepeshkin, and A. R. Oganov (2023). Prediction and rationalization of abundant C-N-H molecules in different environments. *J Phys Chem Lett* 14 (37), 8367–8375. https://doi.org/10.1021/acs.jpclett.3c01753.
- E. E. Vaneeva, S. V. Lepeshkin, D. V. Rybkovskiy, and A. R. Oganov (2025). Exploring the diversity of molecular carbon oxides, and their potential as high energy density materials. *Mater. Today Energy* 49 (101821), 101821. https://doi.org/10.1016/j.mtener.2025.101821.
- G. Acke, S. Van Damme, R. W. A. Havenith, and P. Bultinck (2019). Quantifying the conceptual problems associated with the isotropic NICS through analyses of its underlying density. *Phys Chem Chem Phys* 21 (6), 3145–3153. https://doi.org/10.1039/ c8cp07343k.

**Publisher's Note** Springer Nature remains neutral with regard to jurisdictional claims in published maps and institutional affiliations.

Springer Nature or its licensor (e.g. a society or other partner) holds exclusive rights to this article under a publishing agreement with the author(s) or other rightsholder(s); author self-archiving of the accepted manuscript version of this article is solely governed by the terms of such publishing agreement and applicable law.

